WARSAW UNIVERSITY OF TECHNOLOGY Index 351733
FACULTY OF CIVIL ENGINEERING
COMMITTEE FOR CIVIL AND WATER ENGINEERING
POLISH ACADEMY OF SCIENCES ISSN 1230-2945

DOI: 10.24425/ace.2020.134394
ARCHIVES OF CIVIL ENGINEERING
Vol. LXVI ISSUE 3 2020

MITIGATION OF BLAST LOAD RISK ON REINFORCED CONCRETE STRUCTURES CONSIDERING DIFFERENT DESIGN ALTERNATIVES

Y. E. Ibrahim[1], M. Almustafa[2]

The purpose of this study is to investigate a structure's response to blast loading when composite columns are used instead of conventional reinforced concrete (RC) cross sections and when a conventional structure is retrofitted with braces. The study includes conducting dynamic analyses on three different structures: a conventional reference RC structure, a modified structure utilizing composite columns, and a modified structure retrofitted with steel braces. The two modified structures were designed in order to investigate their performance when subjected to blast loading compared to the conventional design. During the dynamic analyses, the structures were exposed to simulated blast loads of multiple intensities using the finite-element modelling software, SeismoStruct. To evaluate their performance, the responses of the modified structures were analyzed and compared with the response of the conventional structure. It was concluded that both the structure with composite columns and the steel brace structure experienced less damage than the conventional model. The best performance was obtained through the steel brace structure.

Keywords: Blast loading, RC frame structure, blast mitigation, composite column

[1] Assoc. Prof., PhD., Department of Engineering Management, Prince Sultan University, Riyadh, 11586, Saudi Arabia, e-mail: yibrahim@vt.edu
[2] Graduate student, Department of Civil and Environmental Engineering, Western University, London, Ontario, Canada, e-mail: malmust4@uwo.ca

1. INTRODUCTION

Blast loading is the result of the detonation of explosive material as well as accidental events of gas explosions [11]. Such relatively instantaneous loading has the capacity to cause significant structural damage and a considerable number of casualties [4]. RC frame structures composed of RC beams, columns, and slabs are one of the most common methods of building in today's industry and provide an effective and efficient form of construction. Conventional RC structures, however, are widely susceptible to damages incurred by blast loading. The damage may be as partial as the failure of a few structural elements, or as severe as the total collapse of the structure [14].

Due to the limitations of the capacity of a conventional RC structure to withstand blast loading, it has become necessary to investigate methods to mitigate the risk of blast loading for such structures. Currently, both experimental and computational methods have been adopted in conducting research to reduce the effects of blast loading [1].

The accuracy of finite element analysis of structures under severe loading when compared to experimental results is usually a major concern. Also, conducting experimental tests on full-scale structure under severe loading is rarely developed because of the cost and difficulties concerned. Accordingly, using detailed finite element analysis to model the whole structures under blast loads is the option selected by many researchers to assure a realistic approximation of structural collapse. Kwasniewski [5] presented a case study of the progressive collapse of an existing 8-story steel framed structure built for fire tests in the Cardington Large Building Test Facility, UK. He used LS-DYNA in order to develop nonlinear dynamic finite element simulations. The predictive capability of computer simulations was evaluated using a hierarchical verification and validation program. The modelling parameters that affect the accuracy of finite element modelling were identified as beam to columns connections and composite slabs.

In a study by Zhang et al [3], concrete filled steel tube columns were subjected to blast loading and analyzed both experimentally and numerically using LS-DYNA. The results concluded that such columns proved to be effective due to their ability to resist flexural loads caused by both static and dynamic loading. Ibrahim et al [15] examined the nonlinear response of 2-D concrete frame structures exposed to blast loading using ABAQUS. The study investigated concrete filled steel columns and steel columns confined by reinforced concrete along with the level of damage incurred upon each

column. It was found that both types of columns improved the overall response of the 2-D frame structure. Other researchers investigated the response of a real 4-story and 6-story reinforced concrete structures under blast load through a finite element analysis conducted on a 3-D model using ABAQUS [6,16]. Out of different alternative designs considered for enhancing the structural response, it was concluded that encasing the exterior columns by steel tubes provides tremendous benefits in reducing the blast risk on this type of structures. Kyei & Braimah [2] studied the response to blast loading of RC columns with adjusted transverse reinforcement spacing using both LS-DYNA and experimental methods. The study resulted in a reduced lateral displacement when subjected to small-scaled explosions. It was also concluded that at similar scaled distances, having a greater charge mass results in a greater lateral displacement of the column.

Among the methods of investigating the field of blast loading effects on structures, experimental methods are both costly and complex to set up. Experimental methods also require a great measure of safety to be taken. Computational methods, however, are a reliable alternative to experimental methods being that they do not require the safety requirements, cost, nor difficulties that experimental methods carry. Finite element methods have proven to be a successful and effective way for researchers to accurately model and analyze structures under numerous forms, conditions, and loadings without the potential limitations that exist in experimental methods [8].

In this paper, the effect of blast loading was analyzed on three distinctive 3D models. The first model acted as a conventional structure in which the second and third models were compared with. The second model was a conventional structure in which the columns were replaced with composite columns. The third model was a conventional structure having been retrofitted with X-oriented steel braces in its frames. The three models were subjected to three different magnitudes of blast loading through a dynamic analysis using SeismoStruct in which the displacement time-histories, energy dissipation represented by elastic hysteretic curves, and the resulting damages of the exposed structures were analysed and compared.

2. MATERIALS AND METHODS

2.1. STRUCTURAL MODELS

All three structures are 3-bay 4-story moment-resisting framed structures with bay width of 4m. The frames are spaced 6m apart from each other. The models consisted only of beams and columns as masonry walls and slabs were found to fail very early under the exposure of blast loading and were therefore not considered. The self-weight of the walls and slabs, however, was considered.

Furthermore, beams of all three structures were modelled having the same reinforcements and cross-sectional area. The elements of the three structural models were modelled as inelastic plastic-hinge frame based elements [10]. The compressive strength of the concrete used was 28 MPa while the yielding stress of the reinforcing steel used was with respect to the Menegotto-Pinto steel model [7]. The concrete was modelled using a uniaxial constant confinement concrete model initially presented by Madas [9]. The model considers confinement effects, which are provided by the lateral transverse reinforcement. The concrete model assumes constant confining pressure throughout the entire stress–strain range.

2.1.1. MODEL 1

The first model is the conventionally constructed model acting as a benchmark for the comparison of performance with respect to the other two models. The structural models and the details for the beams and columns are presented in Figure 1 and Table 1, respectively.

Table 1. Details of Beam Design and Details of Column Design (model 1)

	Dimensions (cm)	Tension Reinforcement	Compression Reinforcement	Transverse Reinforcement	Longitudinal Reinforcement
Beam	60x30	5 ϕ 20	4 ϕ 16	10 ϕ 10/m	--
Column (model 1)	50x40	--	--	10 ϕ 10/m	4 ϕ 20 (corners); 8 ϕ 16 (sides)

2.1.2. MODEL 2

The second model adopts the blast mitigation technique of concrete-filled, steel composite columns. The steel composite column functions to increase the maximum bending capacity of the column as well as increase the column's ability to dissipate energy. The capacity of the axial force of the steel composite column was designed to be similar to that of the conventional column of the first model. The second model maintains the same beam design as the first model with the columns being steel composite columns of dimensions 40x30cm having a steel casing thickness of 5mm. The representation of the second model can be seen in Figure 2.

2.1.3. MODEL 3

The third model utilizes steel braces as an attempt to improve the structure's response to blast loading. The steel braces operate to increase the lateral stiffness of the structure allowing it to dissipate more energy. The third model maintains the same column and beam design as the first model. The design of the third model only accounted for the braces to resist loading in one direction for simplification purposes. The steel brace used was a W6x9 steel beam modelled with released moment offsets. The cross section has a depth of 153.162mm, width of 101.6mm, web thickness of 5.842mm, flange thickness of 7.112mm and a total cross sectional area of 2322.58mm^2. The representation of the third model can be seen in Figure 3.

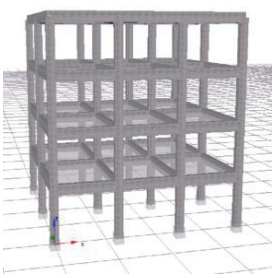

Fig. 1. Conventional RC structure (model 1)

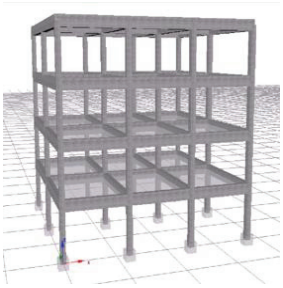

Fig. 2. Composite column structure (model 2)

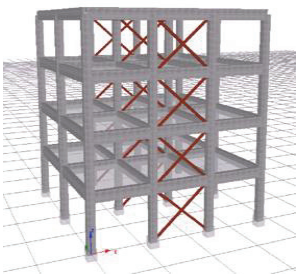

Fig. 3. Steel brace structure (model 3)

2.2. CASES OF BLAST LOAD EXPOSURE

The extent of any blast load depends primarily on the weight of the explosion and the distance between the source of the explosion and the point of impact. The three structural models presented are each subjected to three distinct cases of varying magnitudes. In each case, the weight of the explosive material is kept constant at 0.7 ton (1400 lbs.) of TNT whereas the distance between the source of the blast and the base of the building is decreasing in order to increase the magnitude of the blast. The source of the explosion is assumed to be at ground level and at the center of the building where the blast is directed towards the x-direction in each case.

- Case 1: each model is subjected to 0.7 ton of TNT at a standoff distance of 14m
- Case 2: each model is subjected to 0.7 ton of TNT at a standoff distance of 13m
- Case 3: each model is subjected to 0.7 ton of TNT at a standoff distance of 12m

2.3. BLAST LOAD PARAMETERS AND APPLICATION

The relevant blast load parameters that correspond to the three cases are calculated from the positive phase shock wave parameters for a hemispherical TNT explosion on the surface at sea level established by UFC 3-340-02 [12]. The time history of the blast pressure on the building is calculated from the following equation:

$$P(t) = P_{S0} * (1 - \frac{t}{t_0})e^{\frac{-b*t}{T_0}} \quad (1)$$

where

t_0: the duration of the positive overpressure phase.

b is the waveform parameter.

t_A: the arrival time of the blast front.

t is time measured from the instant that the blast wave arrives (at time = t_A)

P_{S0}: the peak side-on overpressure for positive overpressure calculated from the chart developed for calculating the phase shock wave parameters for a hemispherical TNT explosion on the surface at sea level UFC 3-340-02 [12].

This pressure is calculated based on the scaled distance Z, which is calculated according to the following equation:

$$Z = \frac{R}{W^{\frac{1}{3}}} \quad (2)$$

where

R is the standoff distance between the blast and the node, and

W is the weight of the explosive material

Figure 4 displays an idealized pressure time-history of a shockwave. Throughout the analyses, it was assumed that the arrival time (t_A) of the blast was the same for all nodes given that the alterations were relatively insignificant, and all applied loads due to the blast resulted from the positive phase of the blast. Blast parameters extracted from the chart were used to model the simulated loading as shown in Figure 4. The applied blast loads on the models were modelled as point loads acting on each node from the side of the structure directly exposed to the blast. The parameters were taken with respect the distance between each corresponding node and the source of the blast. Figure 5 represents the nodes from the side of the structure upon which the blast acted.

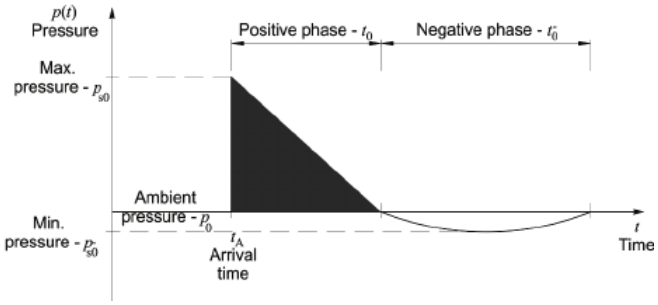

Fig 4. Pressure time-history of a shockwave [15]

The applied point loads on the nodes, denoted F, were calculated by multiplying the peak pressure on each node by the corresponding tributary area. The calculated blast parameters and the force applied to each node of the three cases are shown in tables 2, 3, and 4.

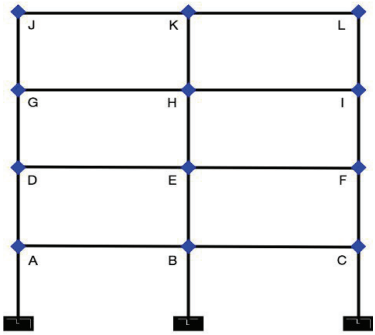

Fig. 5. Node representation of exposed side

Table 2. Blast parameters for each node of case 1 (0.7 ton TNT at standoff 14m)

Node	R (m)	Z (ft/lb$^{1/3}$)	P_{S0} (kPa)	t_0 (msec)	F (kN)
A	15.52	4.4	1378.95	1.7	4964.2
D	16.37	4.64	1275.53	1.7	3826.5
G	17.69	5.02	1034.21	1.7	3102.63
J	19.4	5.5	827.37	1.8	1985.68

Table 3. Blast parameters for each node of case 2 (0.7 ton TNT at standoff 13m)

Node	R (m)	Z (ft/lb$^{1/3}$)	P_{S0} (kPa)	t_0 (msec)	F (kN)
A	14.63	4.15	1792.64	1.7	6453.5
D	15.52	4.4	1379	1.7	4137
G	16.9	4.8	1103.16	1.7	3310
J	18.68	5.3	896.32	1.8	2151.2

Table 4. Blast parameters for each node of case 3 (0.7 ton TNT at standoff 12m)

Node	R (m)	Z (ft/lb$^{1/3}$)	P_{s0} (kPa)	t_o (msec)	F (kN)
A	13.75	3.9	2206.32	1.7	7942.75
D	14.7	4.17	1723.7	1.7	5171.1
G	16.15	4.58	1379	1.7	4137
J	18	5.11	965.26	1.7	2316.6

3. RESULTS AND DISCUSSION

The cases were simulated using nonlinear dynamic time-history analysis using SeismoStruct. In each case, the blast load was calculated using the extracted blast load parameters and the instantaneous loading was applied. Although the actual loading occurs and ends in a very short duration of time (approximately 1.7 msec), each analysis was allowed to continue for 3 seconds in order to examine the structural response as well as the progressive damage of each model. Furthermore, it is noted that the point of reference taken for the computation and collection of data was the farthest node from the blast in the fourth story of each model.

3.1. DISPLACEMENT TIME-HISTORIES AND HYSTERETIC CURVES

The first form of representing the analysis results was the time history of top floor displacement of the models during each case. These results are shown in Figure 6, 8 and 10 for the three cases, respectively. The hysteretic curves of the energy dissipation for the three cases are shown in Figure 7, 9 and 11, respectively.

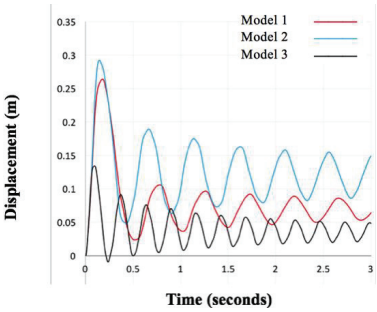

Fig 6. Top floor displacement (case 1)

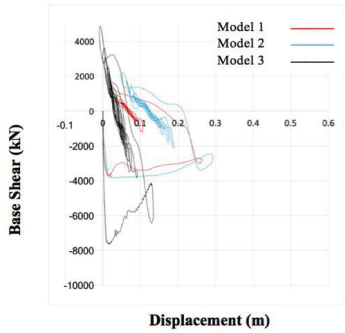

Fig. 7. Hysteretic curve of case 1

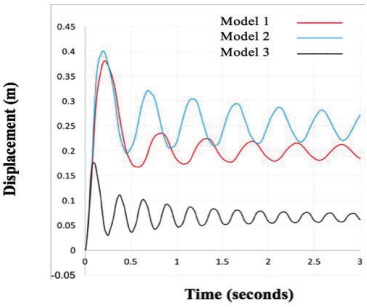

Fig 8. Top floor displacement (case 2)

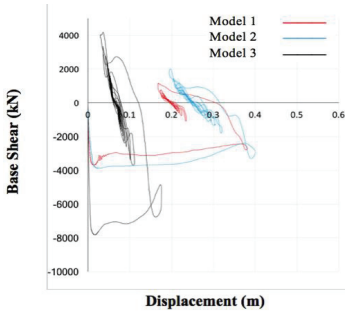

Fig. 9. Hysteretic curve of case 2

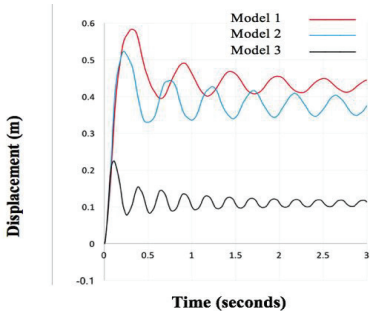

Fig 10. Top floor displacement (case 3)

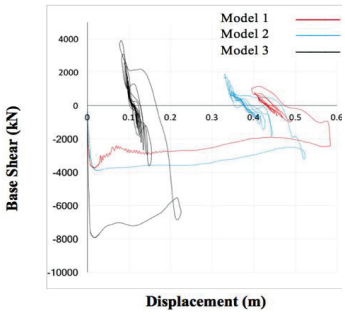

Fig. 11. Hysteretic curve of case 3

According to the results obtained, the highest dissipation of energy displayed in each case was observed within the time in which the blast loading was applied until the maximum displacement was reached. The free vibration response of model 1 and 2 showed similar natural frequency. This was

observed from the time history of top floor displacement after the blast load. This can be easily understood from having almost similar stiffness in both models. However, noticeable smaller frequency is observed in model 3, which can be explained due to the increase of the lateral stiffness of the frame upon the use of steel braces. These observations remained consistent in all scenarios.

In both the first and second cases, model 2 exhibited a higher maximum top floor displacement than model 1 with a higher dissipated energy than model 1. Model 3 had a lower maximum top floor displacement than model 1 with a considerable higher dissipation of energy than model 1. In the third case, model 2 exhibited a lower maximum top floor displacement than model 1, but a greater dissipation of energy than model 1. This comparison was inconsistent with the comparisons made in the first and second scenario. It was found that the higher displacement of model 1 was explained by failures occurring within the elements of model 1. The energy dissipated by model 2, however, was observed to be higher than that of model 1, which remained consistent in all three scenarios.

The residual deformations in model 3 were much less than those developed in model 1 and model 2. In case 3, where the explosive material was at standoff distance of 12m from the structure, the residual deformation was about 0.45m, 0.38m and 0.12m, for the models 1, 2 and 3, respectively. This shows the great enhancement in the structural response under blast loads when the structure is designed with steel braces.

The standoff distance has a considerable effect on the structural response of the three models when subjected to blast loading. Increasing the standoff distance from 12m (case 3) to 14m (case 1) resulted in considerable reduction in the maximum top floor displacement in the three models. The reduction was 53%, 44% and 43% for models 1, 2 and 3 respectively.

3.2. DAMAGE REPRESENTATION

The third form of presenting the results is the investigation of the damages incurred to each model during each case. The types of damages considered ware the following:

- Yielding of steel bars in RC sections
- Crushing of unconfined concrete in RC elements
- Crushing of confined concrete in RC elements
- Exceeding the maximum chord rotation capacity as defined by Mpampatsikos et al [13]
- Fracture in steel bars in RC sections

In the third model, the damages incurred to the braces in the form of yielding or fracturing was also considered. The damage representations of case 1, 2, and 3 are recorded and displayed in Tables 5, 6, and 7, respectively.

Table 5. Damage representation of the models during case 1

	Yield	Unc crush	Conf crush	Chord-rot	Fracture	Brace Yield
Model 1	70	34	5	8	0	-
Model 2	30	43	1	0	0	-
Model 3	68	13	4	1	0	10

Table 6. Damage representation of the models during case 2

	Yield	Unc crush	Conf crush	Chord-rot	Fracture	Brace Yield
Model 1	76	39	17	12	0	-
Model 2	29	43	23	0	0	-
Model 3	69	20	6	4	0	12

Table 7. Damage representation of the models during case 3

	Yield	Unc crush	Conf crush	Chord-rot	Fracture	Brace Yield
Model 1	77	52	30	27	1	-
Model 2	30	43	25	6	0	-
Model 3	70	26	8	11	0	12

It is noted that all maximum chord-rotations occurred in the second model of case 3 were from beam elements and not from the composite column elements. Furthermore, it is noted that in all three cases, none of the composite column elements of model 2 yielded, instead all yielded elements were beams. In comparison to the first model, the second model displayed considerably fewer yielded elements, fewer overall elements which experienced crushed confined concrete, and significantly fewer elements which reached maximum chord-rotation. The second model, however, experienced more overall elements with crushed unconfined concrete. The damages incurred in model 2 are mitigated through fewer crushed cores of concrete, fewer yielded elements, and fewer elements reaching maximum rotation capacity with respect to model 1. In comparison to the first model, the third model had nearly the same number of yielded elements but experienced much fewer instances of both confined and unconfined crushed concrete. The number of elements reaching maximum chord

rotation capacity are also fewer than those of model 1. The mitigated damages to the third model can be explained by the presence of braces, thus the braces experienced yielding. In all three cases, the damages sustained by the structural elements in model 2 were less than those sustained by model 1. Similarly, the structural elements of model 3 exhibited less damage than those in model 1. The only element to experience fracture was in the conventional model.

4. CONCLUSION

The purpose of this study is to investigate a structure's response to blast loading when using composite columns as a substitute to conventional RC columns, and when retrofitted with braces. The models were designed and exposed to three cases of simulated blast loadings of varying intensities during which displacement time-histories, hysteretic curves, and damage representations were obtained. The performance of the two modified models was compared with the performance of the conventional model. The following conclusions were reached:

- The composite column structure, experiencing a higher maximum top floor displacement and higher dissipation of energy, sustained less damage when compared to the conventional structure in case 1 and case 2. In case 3, where the standoff distance was smaller (12.0 m), the conventional structure was subjected to the highest top floor displacement and residual deformations.
- Most of the damages exhibited in the composite-columns structure were in the beams.
- Considering the steel-braced structure, it has higher energy dissipation capacity when compared to both the composite-columns and the conventional structure and accordingly it experienced the least damage of the three models.
- Structural elements that reached the failure stage were no longer able to dissipate more energy.
- The standoff distance has a considerable effect on structural response under blast loads. Increasing the standoff distance from 12m (case 3) to 14m (case 1) resulted in considerable reduction in the maximum top floor displacement in the three models. The reduction was 53%, 44% and 43% for models 1, 2 and 3 respectively. It is highly recommended to take the possible measures to guarantee the maximum possible standoff distance for important structures that might be susceptible to blast threats.

The results are based on approximated blast loads taken at discrete points of the structure and based on the comparisons of performance relative to the conventional model. These aspects may be considered as limitations to the current study which would require a more detailed modelling approach or an experimental program to validate the extent of the stated conclusions. Additionally, further studies of the current investigation include the consideration of bracing location placements and designs, local behavior of individual elements, and local behavior of beam-to-column and brace connections.

ACKNOWLEDGEMENT: Authors would like to express their thanks to Prince Sultan University for supporting the publication of this article.

REFERENCES

1. A. Jacinto, R. Ambrosini, R. Danesi, "Experimental and computational analysis of plates under air blast loading", International Journal of Impact Engineering 25(10): 927-947, 2001.
2. C. Kyei, A. Braimah, "Effects of transverse reinforcement spacing on the response of reinforced concrete columns subjected to blast loading", Engineering Structures 142: 148-164, 2017.
3. F. Zhang, C. Wu, H. Wang, Y. Zhou, "Numerical simulation of concrete filled steel tube columns against BLAST loads", Thin-Walled Structures 92: 82-92, 2015.
4. K. Dai, J. Wang, Z. Huang, H. Felix Wu, "Investigations of structural damage caused by the fertilizer plant explosion at West, Texas. II: ground shock", Journal of performance of constructed facilities 30(4): 04015065, 2015.
5. L. Kwasniewski, Nonlinear dynamic simulations of progressive collapse for a multistory building. Engineering Structures 32(5):1223-1235, 2010.
6. M. Ismail, Y. Ibrahim, M. Nabil, M.M. Ismail, "Response of A 3-D Reinforced Concrete Structure to Blast Loading", International Journal of Advanced and Applied Sciences 4(10): 46-53, 2017.
7. M. Menegotto, P. Pinto, "Method of analysis of cyclically loaded RC plane frames including changes in geometry and non-elastic behavior of elements under normal force and bending", Preliminary Report IABSE 13, 1973.
8. O. Esmaeilnia, S. Mollaei, "Investigation of Axial Strengthened Reinforced Concrete Columns under Lateral Blast Loading", Shock and Vibration, Article ID 3252543, 2017.
9. P. Madas, "Advanced modelling of composite frames subjected to earthquake loading" Thesis (PhD), London, UK, Imperial College, University of London, 1993.
10. Seismosoft, SeismoStruct v7.0 – A computer program for static and dynamic nonlinear analysis of framed structures. Aavailable from http://www.seismosoft.com, 2014.
11. T. Ngo, P. Mendis, A. Gupta, J. Ramsay, "Blast loading and blast effects on structures - An overview", Electronic Journal of Structural Engineering 7: 76-91, 2007.
12. UFC 3-340-02, "Unified Facilities Criteria, Structures to resist the effects of accidental explosions", Department of Defense, USA, 2002.
13. V. Mpampatsikos, R. Nascimbene, L. Petrini, "A Critical Review of the R.C. Frame Existing Building Assessment Procedure According to Eurocode 8 and Italian Seismic Code", Journal of Earthquake Engineering 12: 52-82, 2008.
14. W. Chen, H. Hao, S. Chen, "Numerical analysis of prestressed reinforced concrete beam subjected to blast loading", Materials & Design 65: 662-674, 2015.
15. Y. Ibrahim, M. Ismail, M. Nabil, "Response of Reinforced Concrete Frame Structures under Blast Loading", Procedia engineering 171: 890-898, 2017.
16. Y. Ibrahim, M. Nabil, "Assessment of structural response of an existing structure under blast load using finite element", Alexandria Engineering Journal, 58(4): 1327-1338, 2019

LIST OF FIGURES AND TABLES:

Received 01.12.2019 Revised 15.03.2020